

Versatile Climbing Robot for Vessels Inspection

Mohamed G. Alkalla^{1,a}, Mohamed A. Fanni^{1,b}, and Abdel-Fatah Mohamed^{1,c}

¹ Mechatronics and Robotics Engineering Dept.

School of Innovative Design Engineering, Egypt-Japan University of Science and Technology (E-JUST)
New Borg El-Arab, Alexandria, PO Box: 21934, Egypt.

^{a, b} on leave: Prod. Eng. Mechanical Design Dept., Faculty of Engineering, Mansoura University, Egypt.

^c on leave: Electrical Engineering Department, Faculty of Engineering, Assiut University, Egypt.

e-mail: {mohamed.gouda, mohamed.fanni, abdelfatah.mohamed}@ejust.edu.eg

Abstract—This work focuses on proposing and designing a new climbing robot to explore the interiors of industrial vessels and enables a human outside the vessels to implement required regular inspection tasks efficiently. There are two main adhesion systems in the literature: magnetic and air suction systems. The magnetic system climbs surfaces made of ferromagnetic materials only, while air suction system cannot handle irregular surfaces due to possible seals damage. Opposite to previous climbing robots, the proposed robot here can climb and navigate vessels made from different materials besides handling possible irregular surfaces during inspection. Its main task is visual inspection of welds and any critical spots inside these vessels. The novelty of this robot comes from utilizing a hybrid actuation system. This hybrid actuation system consists of upturned propellers fixed on mobile robot and motorized wheels of the mobile robot. The pressure generated from the upturned propellers increase the friction force between the wheels of the mobile robot and the wall. The wheels' motors generate the required torque either to fix the robot in any position or to move it to any place. Since the motion of the robot comes mainly from the motorized wheel, the stability of the system during navigation is guaranteed. Size and topology optimizations are carried out to achieve optimum design of the proposed robot. Simulation results of the designed robot using ADAMS software prove its feasibility.

Keywords-climbing robot; propeller; hybrid actuation system; adhesion system

I. INTRODUCTION

The systems which have a capability of climbing vertical structures or navigate inside tanks and vessels have an increasing importance in the last two decades. Most of those research groups started in the 90's and developed first prototypes which are able to climb on vertical walls. The application fields are ranging from welding of ship hulls to the inspection of steel bridge or nuclear power plants. Common systems such as 'Rest' which uses six legs and magnetic pads for climbing [1], are applied for such tasks. It is realized that such climbing systems are mainly adopted in places which cannot be reached by humans, where the direct access for the human is too expensive and dangerous. Almost all climbing robots are depending on two main systems (locomotion and adhesion system) to keep the robot attached to the vertical structures. The climbing robot needs

to be designed based on the desired functions and field of applications and these aspects define which locomotion and adhesion principle are needed. There are many locomotion principles such as wheels [2], track systems, sliding frames [3], arms and legs [4]. Each locomotion system depends on the nature of the surface which these robots are moving on and each one has an advantage over the others at certain requirements, see [5]. There are many adhesion systems such as magnetic, pneumatic, mechanical, electrostatic and chemical adhesion systems. The last two adhesion systems are less common than the others. The magnetic adhesion system depends on the magnetic force between the robot and the climbed structures. It is used only for the ferromagnetic material structures. Some climbing robots make use of this adhesion system as Rvc robot [6], see Fig. 1. The second common type of adhesion system is a pneumatic system which depends on air suction. The attraction force between the robot and the wall is proportional to the pressure difference between the pressure chamber or suction cup and the atmosphere. There are a lot of climbing robots make use of this principle such as a known wheeled system (Bigfoot), which uses the chamber sealing as support against tilt [7], as shown in Fig. 2.



Figure 1. Reconfigurable vertical climber (RVC) using magnetic pads.

This pneumatic adhesion type is used for flat and even surfaces. The third common one depends on mechanical grippers and claws which are used for rough surfaces, such as RISE robot [8]. A simple survey on the common climbing robots is presented in [5].



Figure 2. Bigfoot wheeled system climbing robot with air suction.

II. THE PROPOSED CLIMBING ROBOT

A novel climbing robot is proposed here which can overcome a lot of difficulties that faced the previous climbing robots such as: Is the vessel material ferrous or not? Is the surface even or not? These aspects will not be a problem in this proposed robot design, since it depends on upturned propellers mounted on mobile robot. This idea is opposite to flying concept. The propeller here is supposed to push and generate normal force against the vessel wall. A propeller system which is used only for driving a climbing robot is presented in [9] and [10]. The navigation stability was a major problem in this idea [5]. The proposed idea here is based on a hybrid actuation system which utilizes both upturned propeller thrust force and wheels-motors torque as adhesion system, while utilizes its wheels as locomotion system. So, this proposed robot integrates propellers' system with mobile robot for climbing any vertical/inclined surface in a stable manner and can also hang on ceiling for various inspection tasks. Since the proposed adhesion mechanism does not depend on a magnetic force or air suction which needs sealing means, the proposed robot can climb walls made of arbitrary materials and can handle any obstacles that can damage the seals of air suction robots if they were used. The proposed climbing robot will be introduced here beginning with conceptual design that suggest different wheels/propellers arrangements in Section III. The detailed mechanical design will follow for the best concept in Section IV where the optimum size and topology of the robot structure as well as proper selection of wheels, propellers and motors are carried out. Dynamic simulation using ADAMS for the proposed system will be accomplished in Section V.

III. STRUCTURAL DESIGN OF THE PROPOSED CLIMBING ROBOT

In this section, the novel versatile inspection robot for industrial vessels (VIRIV) is going to be designed. This climbing robot will transmit all vision data to the human outside vessels to enable him to analyze and make a proper decision. The proposed robot uses hybrid actuation system consisting of propellers and motorized wheels' system which signalized the novelty of this climbing robot. Three conceptual designs for the versatile inspection robot are generated. Model 1 is designed with one propeller, two motorized wheels, and two free omni-directional wheels. The drag torque of the propeller is overcome by the frictional

force acting on the motorized wheels. The advantage of this model is that the robot have only three actuators (one for propeller and two for wheels), see Fig. 3. Model 2 is designed with two coaxial propellers (one right-handed, other left-handed) turn in opposite directions. In addition to two driving motorized wheel and two omni-wheels. In this case the drag torques generated from the two propellers eliminate each other. The advantage of this model is its simple mathematical model and greater normal force against wall compared to model 1, see Fig. 4. Finally, in model 3, the two right wheels are driven by one motor while the left two wheels are driven by another motor using timing belts as shown in Fig. 5. The advantage of this conceptual design is the high frictional forces at the four wheels that can be used for climbing. Two coaxial propellers are used with this design in order to obtain a higher thrust force. This model also can be designed using one propeller instead.

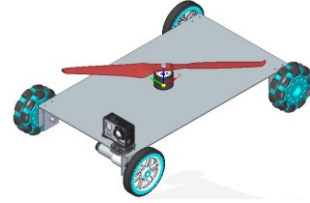


Figure 3. Model 1, with two motorized, two omni-wheels and one rotor.

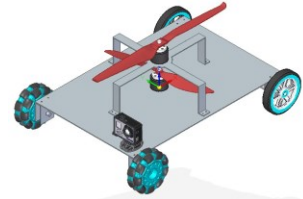


Figure 4. Model 2, with two motorized wheels, omni-wheels and 2 rotors.

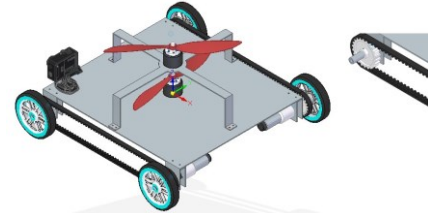


Figure 5. Model 3, with four motorized wheels, timing belts and 2 rotors.

It seems that the third model is the best one due to its preceding advantages. Mechanical design of the robot will be carried out and utilizes the static and dynamic equations. The propellers' normal forces that are exerted on the robot top surface, robot's weight, torque applied on each wheel and the coefficient of friction between wheels' tires and climbing surface are taken into consideration. At any position inside the vessel, the thrust force exerted from the propeller is always normal to the vessel wall while the weight of the robot is vertically downward. Fig. 6 shows all forces acting on the robot chassis and the wheels. N_i and F_f are the normal and frictional forces acting on the wheel i respectively, F_N is the propellers' thrust force acting on robot chassis, a and h are length and width of the chassis, b is the distance between

thrust force F_N and the front wheel axes, c is the distance from chassis centroid to front wheel axes in longitudinal direction, d is normal distance from centroid to a plane contains wheels axes, e is the distance between the centroid and the right wheels in the lateral direction and R is the wheel radius.

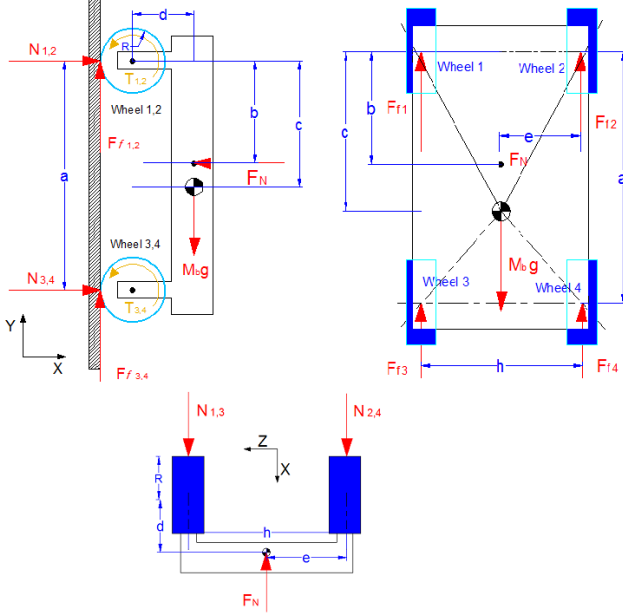


Figure 6. Free body diagram of the robot chassis and wheels.

The static equations which hold the robot on the vertical wall are driven below:

$$N_1 + N_2 + N_3 + N_4 = F_N \quad (1)$$

$$F_{f1} + F_{f2} + F_{f3} + F_{f4} = W \quad (2)$$

$$-(F_{f1} + F_{f3}) \cdot (h - e) + (F_{f2} + F_{f4}) \cdot e = 0 \quad (3)$$

$$(N_1 + N_3) \cdot (h - e) + (N_2 + N_4) \cdot e = 0 \quad (4)$$

$$-(N_1 + N_2) \cdot c - W(R + d) + F_N(c - b) + (N_3 + N_4)(a - c) = 0 \quad (5)$$

It is found that the torque T_i and frictional forces at front and rear wheels are equals in each side so,

$$F_{f1} = F_{f3} \quad (6)$$

$$F_{f2} = F_{f4} \quad (7)$$

There are seven equations while eight unknowns should be determined. Another equation for N_1 , N_2 , N_3 and N_4 may be added for solving these equations. Using force displacement method for compatibility of the rigid chassis, thus, the last equation will be as follows:

$$\frac{N_1}{k_{w1}} - \frac{N_2}{k_{w2}} - \frac{N_3}{k_{w3}} + \frac{N_4}{k_{w4}} = 0 \quad (8)$$

where, k_{wi} is the stiffness of wheel i , the frictional force F_f should always be less than the normal force N_i multiplied by

the wheel's coefficient of static friction μ_s to prevent the slippage, as in (9). The wheels torques are defined from (10).

$$F_f \leq \mu_s \cdot N_i \quad (9)$$

$$T_i = F_f \cdot R \Rightarrow i = 1 \dots 4 \quad (10)$$

It was found that the suitable design of proposed robot should have sufficient friction on the whole wheels to support the weight of the robot and hold it to the wall especially in vertical position.

IV. STRUCTURAL OPTIMIZATION

A detailed design is carried out to determine the sizes, dimensions and specifications of the motors, propellers and wheels as well as type of the material used for chassis. Also structural optimization such as size and topology optimization are applied for the chassis to obtain a light-weight climbing robot.

A. Size Optimization based on Weight Minimization

Size optimization technique is applied for the system to optimize the robot weight which is an important issue for such climbing robots in order to make it as light as possible. There are many constraints for the optimization such as the rotor thrust force which is limited to 3 kg for each rotor. Also there are the motors whose rated maximum torques are proportional with its sizes and weights. On the other hand there is a relation between maximum frictional force on the wheel and the normal force acting on it, as in (9). Thus, it is a complicated optimization problem which should be solved. The problem depends on continuous values of some parameters such as dimensions of chassis and discrete values of other parameters such as maximum motors torque, maximum rotors' thrust force or propellers diameters.

$$\min_x : W_T = (a \cdot h \cdot t) \cdot \rho g + W_a \quad (11)$$

$$s.t. : F_f \leq \mu_s N_i \quad (12)$$

$$F_N \geq W_T / \mu_s \quad (13)$$

$$T_1 + T_3 \leq T_{\max} \quad (14)$$

$$T_2 + T_4 \leq T_{\max} \quad (15)$$

$$a, h \geq D_p \quad (16)$$

$$D_p / 2 \leq b \leq (a - D_p / 2) \quad (17)$$

$$N_i \geq 0 \quad (18)$$

$$\delta \leq \delta_{\max} \quad (19)$$

$$\sigma \leq S_y / F_s \quad (20)$$

The objective function is minimization of the total robot weight W_T subjected to some constraints as illustrated above in (11) to (20) and all these constraints should satisfy equations (1) to (8). W_a is a payload weight consists of all components of the robot except the chassis weight such as

(motors, wheels, rotors, propellers, controllers, pulleys, belts and camera). t , ρ are thickness and density of the chassis respectively. T_{max} is the maximum torque applied by wheels' motors and D_p is propeller diameter. δ , δ_{max} are the deflection of the chassis and maximum allowable deflection respectively. σ , S_y and F_s are the maximum stress of chassis, yielding strength of chassis material and factor of safety respectively. The design variables are a , h , b , d and R . The initial design parameters are shown in Table I, where F_N is taken according to the maximum allowable thrust force generated by the two rotors which is 5 kg at the normal load current. The smallest propeller diameter that will be suitable for the selected rotor and generate the required thrust load is 12 inch.

TABLE I. INITIAL DESIGN PARAMETERS FOR SIZE OPTIMIZATION (ALUMINUM 6061-T6 WITH 2 MM THICKNESS)

Initial Design Parameters	Values
Payload weight W_a	1 kg
Rotors thrust load F_N	5 kg
Density ρ	2700 kg/m ³
Coefficient of static friction μ_s	0.4
Max. motor torque T_{max}	0.5 N.m
Propeller diameter D_p	12" or 0.31 m
Max. allowable deflection δ_{max}	3 mm
Yielding strength S_y	105 Mpa
Modulus of elasticity E	70 Gpa
Factor of safety F_s	1.5
Initial chassis size ($a \times h$)	0.40 × 0.40 m

TABLE II. FINAL RESULTS OF THE ROBOT CHASSIS SIZE OPTIMIZATION

Optimum Parameters	Values
a, h, b, d, R	0.35, 0.35, 0.175, 0.02, 0.05 m
Maximum stress σ	58.331 Mpa
Deflection δ	1.9 mm
Normal force $N_1 = N_2$	11.095 N
Normal force $N_3 = N_4$	13.422 N
Friction force $F_{fl,2,3,4}$	4.0736 N

The MATLAB optimization toolbox is used while ANSYS is used for a finite element analysis to obtain the chassis deflections and stresses. The lower bound values for a , h , b , d and R , are D_p , D_p , $D_p/2$, 0.02 and 0.05 m respectively while the upper values are 0.6, 0.6, (0.6- $D_p/2$), 0.1 and 0.1 m. The optimization process results in an optimum chassis size of 0.35×0.35 m with a total final weight of 1.661 kg while the initial design was 1.864 kg, also the final deflection is 1.9 mm which is less than the initial value. The suitable wheel radius is 5 cm, for assembling the wheels' motors easily and make a small gap between robot and vessels in order to overcome obstacles. The final results of the size optimization are shown in Table II.

B. Topology Optimization based on Compliance Minimization

Topology optimization technique is used for optimizing the robot chassis and minimize its compliance. A continuous relative density x_i is used as a design variable. The topology optimization is mainly based on a penalization concept of the

intermediate densities of the material to be solid or void as in (22):

$$\rho_i(x_i) = \rho_0 x_i \quad (21)$$

$$E_i(x_i) = E_0 x_i^p \quad (22)$$

$$0 < x_i \leq 1 \quad (23)$$

where, ρ_i and E_i are element density and modulus of elasticity respectively. ρ_0 and E_0 are the initial density and elasticity of the base material. p is a penalization power usually equals 3. Topology optimization is accomplished using the method of moving asymptotes (MMA) inspired by Svanberg in [11] using MATLAB code. This optimization problem is based on compliance minimization as illustrated in (24) to (27).

$$\min_x : C(x) = U^T K U = \sum_{i=1}^n (x_i)^p u_i^T k_i u_i \quad (24)$$

$$s.t. : \frac{V(x)}{V_0} = V_{frac} \quad (25)$$

$$: KU = F \quad (26)$$

$$0 < x_{min} \leq x \leq 1 \quad (27)$$

where, U and F are the global displacement and force vectors, respectively; K is the global stiffness matrix, u_i and k_i are the element displacement vector and stiffness matrix, respectively. $V(x)$ and V_0 are the material volume and the initial volume respectively; where V_{frac} is the prescribed volume fraction. For more details on topology optimization technique, see [12]. The initial design model with boundary conditions and loads is shown in Fig. 7.

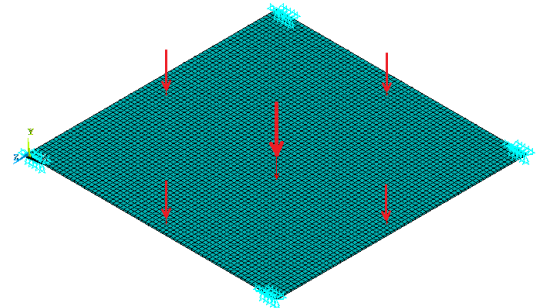


Figure 7. Initial design of robot chassis with boundary conditions and loads modeled by ANSYS.

The topology optimization technique generates holes with various shapes and sizes within the robot chassis, as shown in Fig. 8. The final results for topology optimization is shown in Table III at initial design variables x_0 and volume fraction equals 0.65. The deflection of the final design does not exceed the initial design and also does not exceed the maximum deflection limit of 3 mm. A light weight and higher strength material for chassis such as carbon fiber shall also be used alternatively. The final topological deign is modeled using Solid Edge ST6 software and also a finite element analysis is applied for studying the critical regions in the robot chassis.

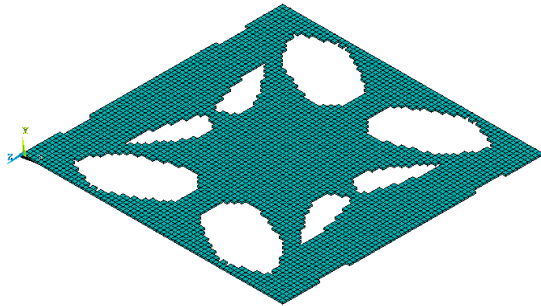


Figure 8. Final Topological optimum design of VIRIV robot chassis.

TABLE III. RESULTS OF ROBOT CHASSIS TOPOLOGY OPTIMIZATION

Properties	Compliance (N.m)	Max. Defl. (mm)	Max. Stress (Mpa)
Initial Design	0.278845	2.9691	58.3314
Topological Design	0.113703	2.6615	67.7983

Finite element analysis could be used to check either the robot body design is safe or not and study the critical regions within the design to modify it. The stress analysis of the final chassis design shows that the maximum stress is 65.3 Mpa less than allowable one. This maximum stress occurs at the sharp corners between chassis and the wheel support. So these corners are recommended to be modified to round corners with radius 30 mm to reduce the concentrated stresses. Consequently the maximum stress is decreased to 38.9 Mpa at these round corners. It is safer than the sharp corners, as shown in Fig. 9.

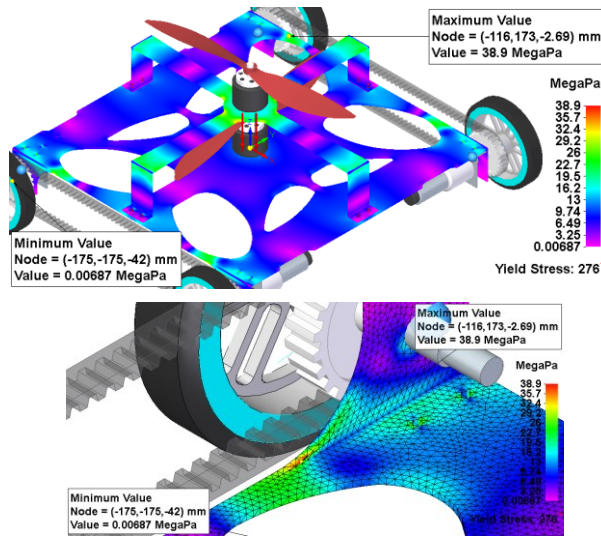


Figure 9. FEA using Solid Edge for VIRIV Robot chassis with 30 mm round corners.

V. RESULTS

Dynamic simulation for the climbing robot is applied using MSC ADAMS software. Rotors thrust load of 5 kg (49.03 N) is applied on the model, each wheel is actuated using a torque equals to 0.2036 N.m and the whole robot weight is 1.661 kg as mentioned before in section IV. The

motion is modeled with an aid of special contact forces between the four wheels and the vertical wall surface or the vessel's inner surface, besides rolling of these wheels due to the actuating torque on it. The static and dynamic coefficient of friction are specified as 0.4 and 0.3 respectively, the stiffness of the wheels is 10^5 N/mm , the force exponent is 3 and the damping coefficient is 10^4 N.s/mm , while penetration depth is determined as 2 mm . Also the stiction transition velocity and the friction transition velocity are equal to 0.1 mm/s and 100 mm/s respectively. These values are used as the contact parameters in ADAMS software. The climbing robot model is theoretically tested on both a vertical wall and inside a vessel with a diameter of 5 m .

A. Vertical Model

Firstly, the climbing robot model is tested by ADAMS at the specified torque and normal force which specified above. The model at these values remains in its position on the vertical wall without any forward or backward motion. When the torque value increases a little bit to become 0.206 N.m , as shown in Fig. 10, the robot begins to climb the wall and goes upward in the vertical direction. The position, and linear velocity of the center mass of platform in y -direction varying with time is shown in Fig. 11.

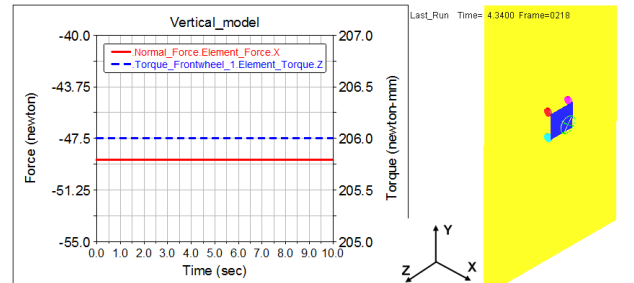


Figure 10. The wheels torque and the rotors thrust force of climbing robot.

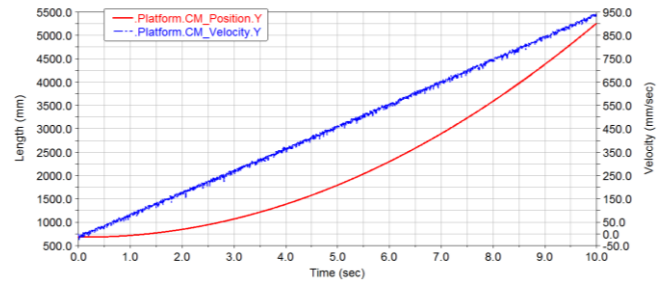


Figure 11. The vertical position and linear velocity of the platform in y -direction varying with time.

B. Vessel Model

The second simulation is climbing the inner cylindrical surface of a vessel with diameter 5 m , as shown in Fig. 12. All kinematic and dynamic information of the robot and its components (i.e. chassis and wheels), can be obtained at any specific time. It is found that at the same thrust force 49.03 N , the torque on each wheel can decrease to 0.180 N.m and still climb the interior surface of vessel. The thrust force in x , y directions, its magnitude and also the front wheel torque

about its axis is shown in Fig. 13. The motion of the robot begins from the bottom of the vessel and the robot moves on the inner cylindrical surface to climb the vessel. The robot reaches the maximum vertical position on the vessel's ceiling at a time nearly equals 2.5 sec and goes down again in a circular path. The position in x , y directions and the linear velocity magnitude of the robot are shown in Fig. 14.

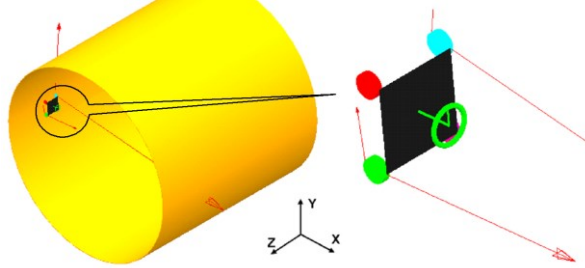


Figure 12. Modelling and simulation of the climbing robot inside vessel using ADAMS.

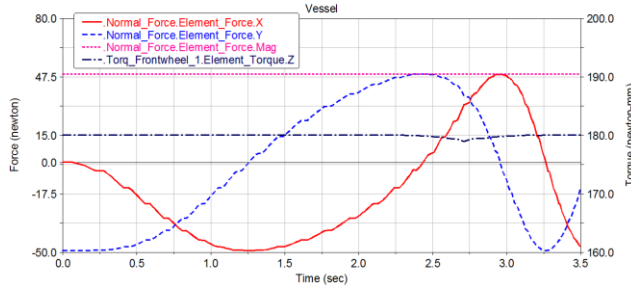


Figure 13. The wheel torque and the rotor thrust force of the climbing robot varying with time.

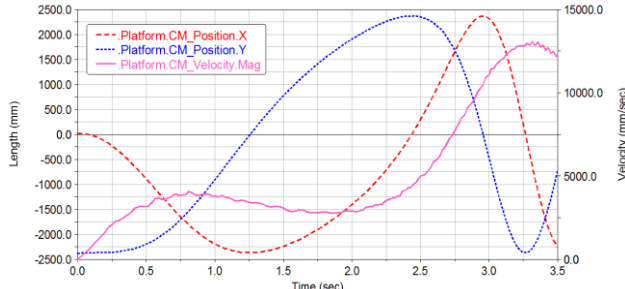


Figure 14. Robot chassis position in x and y directions and linear velocity magnitude of the robot varying with time.

VI. CONCLUSIONS

The paper presents a new kind of climbing robot which can inspect petrochemical tanks and vessels without any restrictions on the climbing surface material or obstacles inside them. The new concept of climbing by a hybrid system, which consists of propellers and motorized wheels, is approved using MSC ADAMS software. Both size and topology optimization are applied to obtain a light weight robot. The stability of the overall system during navigation is guaranteed by using such hybrid system. The simulation shows that there is a good harmony between the thrust forces

and the wheels' torques. The linear velocity of the robot is required to be constant for regular movement. This task needs motion control which will be accomplished in the future work.

ACKNOWLEDGMENT

The first author is supported by a scholarship from the Mission Department, Ministry of Higher Education (MOHE), Egypt, which is gratefully acknowledged. The authors are grateful to Professor Krister Svanberg, from the Royal Institute of Technology, Stockholm, for providing us with method of moving asymptotes code.

REFERENCES

- [1] J. Grieco, M. Prieto, M. Armada, and P. de Santos, "A six-leggedclimbing robot for high payloads," in Proc. the 1998 IEEE International Conference on, vol. 1, pp. 446-450, Sep 1998.
- [2] B. Bridge, J. Shang, B. Bridge, T. Sattar, S. Mondal, and A. Brenner, "Development of a climbing robot for inspection of long weld lines," Industrial Robot: An International Journal, vol. 35, no. 3, pp. 217-223, 2008.
- [3] V. Gradetsky and M. Knyazkov, "Multi-functional wall climbing robot," in Proc. Adaptive Mobile Robotics,Proceedings of the 15th International Conference on Climbing and Walking Robots, CLAWAR, Baltimore, USA, 2012, pp. 807-812.
- [4] S. Kim, M. Spenko, S. Trujillo, B. Heyneman, V. Mattoli, and M. Cutkosky, "Whole body adhesion: Hierarchical, directional and distributed control of adhesive forces for a climbing robot," in Proc. 2007 IEEE International Conference on Robotics and Automation, April 2007, pp. 1268-1273.
- [5] D. Schmidt and K. Berns, "Climbing robots for maintenance and inspections of vertical structures—A survey of design aspects and technologies," Robot. Auton. Syst., vol. 61, no. 12, pp. 1288-1305, Dec. 2013.
- [6] G. Peters, D. Pagano, D. K. Liu, and K. Waldron, "A prototype climbing robot for inspection of complex ferrous structures," in Proc. the 13th International Conference on Climbing and Walking Robots and the Support Technologies for Mobile Machines, Nagoya, Japan, 2010, pp. 150-156.
- [7] T. White and D. Cooke, "Robosense—Robotic delivery of sensors for seismic risk assessment," in Proc. International Conference on Climbing and Walking Robots, CLAWAR, Madrid, Spain, 2000, pp. 847-852.
- [8] M. J. Spenko, G. C. Haynes, J. A. Saunders, M. R. Cutkosky, A. A. Rizzi, R. J. Full, and D. E. Koditschek, "Biologically inspired climbing with a hexapedal robot," J. Field Robot., vol. 25, no. 4-5, pp. 223-242, Apr. 2008.
- [9] A. Nishi and H. Miyagi, "Propeller type wall-climbing robot for inspection use," in Proc. 10th Int. Symp. on Automation and Robotics in Construction (ISARC), pp. 189-196, 1993.
- [10] A. Nishi, H. Miyagi, and K. Ishihara, "Development of wall inspection robots," in Proc. 12th Int. Symp. on Automation and Robotics in Construction (ISARC), pp. 103-108, 1995.
- [11] K. Svanberg, "The method of moving asymptotesa new method for structural optimization," International Journal for Numerical Methods in Engineering, vol. 24, no. 2, pp. 359-373, 1987.
- [12] M. P. Bendsoe and O. Sigmund, "Topology optimization – Theory, methods and applications, handbook," Springer-Verlag Berlin Heidelberg, 2003, pp. 1-13.